

Original Article

Expression of microRNA-514a-5p and its biological function in experimental pulmonary thromboembolism

Yuanyuan Sun^{1*}, Xingguo Zhang^{2*}, Hua Gao³, Mingjie Liu¹, Qi Cao⁴, Xinyang Kang⁵, Yusheng Wang¹, Ling Zhu¹

Departments of ¹Respiratory Medicine, ²Emergency, ³Clinical Laboratory, Shandong Provincial Hospital Affiliated to Shandong University, Jinan 250000, Shandong, China; ⁴Department of Respiratory Medicine, Shandong Provincial Third Hospital, Jinan 250031, Shandong, China; ⁵Department of General Surgery, The Hospital of China National Heavy Duty Truck Group Company, Jinan 250031, Shandong, China. *Equal contributors.

Received May 13, 2019; Accepted August 12, 2019; Epub September 15, 2019; Published September 30, 2019

Abstract: It is difficult to diagnose pulmonary thromboembolism (PTE) in clinical practice. While microRNAs (miRNAs) have been widely investigated as biomarkers for various diseases, their value as biomarkers for PTE remains largely unknown. In the present study, 83 miRNAs showed altered expression in an intermediate-risk PTE group when compared with their expression in a low-risk PTE group as detected by miRNA microarray analysis. After reviewing those data, hsa-miR-514a-5p was selected as a potential biomarker for PTE progression. Disordered myocardial fibroblast arrangements, broadened intercellular spaces, diapedesis of erythrocytes, and lower numbers of nuclei in the right ventricular wall were observed in rats in a PTE model group when compared to rats in a normal saline (NS) group. Furthermore, hyperexpression of miR-514a-5p exacerbated the morphological characteristics of lung and right ventricular tissues, and caused increased RVHI and lung index values, as well as increased BNP and NT-pro-BNP levels in the PTE model rats, possibly by downregulating Chordin-like 1 (CHRDL1) expression. These results suggest that miR-514a-5p helps to exacerbate PTE development by promoting several aspects of PTE pathology, including inflammation, lung injury, and right ventricular hypertrophy by targeting CHRDL1.

Keywords: Pulmonary thromboembolism, miRNA microarray, miR-514a-5p, CHRDL1

Introduction

Pulmonary thromboembolism (PTE) is a common medical condition associated with significant rates of morbidity and mortality caused by hypercoagulability, endothelial damage, and systemic inflammation [1]. Although diagnostic, anticoagulation, and interventional clot-burden reduction strategies have been the focus of clinical research and care for PE patients, appropriate risk stratification is crucial for selecting the correct treatment for those patients after a prognosis is established [2]. Several key indicators are used for risk stratification of PTE, including hemodynamic parameters, the simplified pulmonary embolism severity index (sPESI), as well as B-type natriuretic peptide (BNP) and N-terminal-proBNP levels, especially for PTE patients with right ventricular dysfunction (RVD) [3-5]. We previously confirmed that the incidence of PTE mortality and adverse events dur-

ing a 14-day prognostic period was significantly higher among patients with RVD than among patients without RVD [6]. Unfortunately, the value of a prognosis for patients with PTE remains controversial, because of none of the indicators are specific for PTE [7]. Therefore, there is an urgent need to identify specific prognostic assessment markers that will enable the precise clinical management of PTE.

MicroRNAs (miRNAs) comprise a class of endogenous RNAs that contain ~22 nucleotides. These miRNAs are capable of binding to the "seed sequences" in the 3'UTR of their target mRNAs to drive either RNA translation or degradation [8]. miRNAs can influence multiple biological processes, including cellular growth, differentiation, apoptosis, and embryonic development [9]. Increasing evidence indicates that miRNAs can play important roles in diagnosing PTE [10-13]. For example, Chen et al [14] found

The role of miR-514a-5p in pulmonary thromboembolism

Table 1. Primers used in the experiments

ID	Sequence (5'-3')
U6 F	CTCGCTTCGGCAGCAC
U6 R	AACGCTTCACGAATTTGCGT
ALL R	CTCAACTGGTGTCTGCGTGG
hsa-miR-514a-5p RT	CTCAACTGGTGTCTGCGTGGAGTCGGCAATTCAGTTGAGCATGATT
hsa-miR-514a-5p F	ACACTCCAGCTGGGTACTCTGGAGAGTGACAA
hsa-miR-369-3p RT	CTCAACTGGTGTCTGCGTGGAGTCGGCAATTCAGTTGAGAAAGATC
hsa-miR-369-3p F	ACACTCCAGCTGGGAATAATACATGTTGATC
hsa-miR-885-3p RT	CTCAACTGGTGTCTGCGTGGAGTCGGCAATTCAGTTGAGTATCCACT
hsa-miR-885-3p F	ACACTCCAGCTGGGAGGCAGCGGGGTGTAGTG
hsa-miR-1304-5p RT	CTCAACTGGTGTCTGCGTGGAGTCGGCAATTCAGTTGAGCACATCTC
hsa-miR-1304-5p F	ACACTCCAGCTGGGTTTGTAGGCTACAGTGAGA
hsa-miR-147b RT	CTCAACTGGTGTCTGCGTGGAGTCGGCAATTCAGTTGAGTAGCAGAA
hsa-miR-147b F	ACACTCCAGCTGGGGTGTGCGGAAATGCTTCT
hsa-miR-323b-5p RT	CTCAACTGGTGTCTGCGTGGAGTCGGCAATTCAGTTGAGTGCGAACT
hsa-miR-323b-5p F	ACACTCCAGCTGGGAGGTTGTCCGTGGTGAGT
GAPDH F	CCTCGTCTCATAGACAAGATGGT
GAPDH R	GGGTAGAGTCATACTGGAACATG
CHRD1 F	TTGTGGTCTCAAGACTTGCC
CHRD1 R	CCCTGATGCTTGCTGAGAAT

that susceptibility to chronic thromboembolic pulmonary hypertension may be conferred by miR-759 via its targeted interaction with the polymorphic fibrinogen alpha gene. Moreover, reduced levels of let-7b might be involved in the pathogenesis of chronic thromboembolic pulmonary hypertension by affecting ET-1 expression [15]. It has been demonstrated that serum microRNA-1233, microRNA-134, and miR-28-3p can serve as specific biomarkers and potential plasma biomarkers for use in diagnosing acute pulmonary embolism [16-18]. These findings provide a scientific basis for the important value of miRNAs in establishing a prognosis for PTE patients. However, little is known about the function of miRNA in PTE. Therefore, exploring the key functions of miRNAs in PTE is of great significance for the treatment of PTE patients.

In the present study, a miRNA microarray analysis was conducted on tissues from 5 low-risk PTE patients, 5 intermediate-risk PTE patients and 5 control subjects. MiR-514a-5p, which showed higher levels of expression in the intermediate-risk PTE group than in the low-risk PTE group, was selected for further analysis. The function of miR-514a-5p in PTE and its molecular mechanism were studied not only to obtain

a better understanding of its mechanism in intermediate-risk PTE, but also to understand its value as a possible target for intervention.

Materials and methods

Patients and control groups

This study enrolled 10 patients who had been diagnosed with PTE (location of the embolism in the pulmonary trunk) by CT-pulmonary angiography [21]. These 10 PTE patients were assigned to a low-risk PTE group (n=5) and an intermediate-risk PTE group (n=5), respectively, based on current risk

stratification guidelines. In brief, low-risk PTE was confirmed when all markers of right ventricular dysfunction and myocardial injury were negative. Intermediate-risk PTE was confirmed when at least one right ventricular dysfunction marker or one myocardial injury marker was positive. For comparison, we also enrolled 5 age- and sex-matched healthy control subjects. Clinical tissues were collected from PTE patients. Adjacent normal clinical tissue specimens were obtained from locations far from the area of inflammation caused by PTE. Twenty pairs of diseased and adjacent normal clinical tissue specimens were analyzed by real-time quantitative PCR (RT-qPCR) for validation purposes. The protocol for this study was approved by the Medical Research Ethics Committee of Shandong Provincial Hospital, and each enrolled patient provided their written informed consent for study participation.

Blood collection and RNA isolation

Samples of blood (3-5 mL each) were collected into EDTA-K2 tubes and mixed by upside down rotation. After a two-step centrifugation process (1700 g at 4°C for 10 min, followed by 2000 g at 4°C for 10 min), the supernatant fractions were transferred into RNase/DNase-

The role of miR-514a-5p in pulmonary thromboembolism

Table 2. Clinical data for the PTE patients and control subjects

PTE Samples	Age	Sex	NT-Pro BNP	Medical history
Intermediate-risk	52.6±8.5	3 ^a /2 ^b	2084.3±297.7	None
Low-risk	56.6±7.5	1 ^a /4 ^b	37.4±5.8	None
Control	53.4±5.7	2 ^a /3 ^b	35.1±5.2	None

Note: a, male; b, female.

free tubes and stored at -80°C until further analysis. The total RNA was extracted from the plasma using Trizol reagent (Invitrogen, Carlsbad, CA, USA) and purified using a RNeasy Mini Kit (Qiagen, Hilden, Germany) according to the manufacturer's instructions for plasma samples.

MiRNA chip

After quality testing, the extracted total RNA was labeled with reagents in a miRCURYTM Array Power Labeling kit (Cat #208032-A, Exiqon), and then detected with a visible spectrophotometer (NanoDrop 1000; Thermo Fisher Scientific, Waltham, MA, USA). Next, the labeled samples were hybridized using a miRCURYTM LNA Array (v.19.0, Exiqon) chip. After being washed with reagents in a wash buffer kit (Exiqon, Copenhagen, Denmark), the hybridized chips were scanned using an Axon GenePix 4000B microarray scanner; after which, the scanned images were processed using GenePix Pro 6.0 image software (Axon Instruments, San Jose, CA, USA). For each type of miRNA, multiple probes were spotted on the array, and the average intensity of those probes was calculated to represent the expression level of a specific miRNA. The relative expression levels of all the differentially expressed RNAs were then clearly displayed on a hierarchical clustering heat map. The differentially expressed miRNAs were statistically analyzed by using the one way ANOVA paired method. The thresholds for up- and down-regulated miRNAs were a +1.5-fold and -1.5-fold change, respectively, and a *p*-value < 0.05.

Validation of the microarray results

Among all the miRNAs detected by microarray assays, a total 6 miRNAs, (miR-514a-5p, miR-369-3p, miR-885-3p, miR-1304-5p, miR-147b, and miR-323b-5p) were selected for further validation by RT-qPCR. Briefly, the extracted RNA was reverse transcribed to cDNA. The specific primers were designed using Primer 5.0 software and synthesized by the Shanghai

Kangcheng Biotechnology Company. Realtime PCR was performed on a Stratagene Mx3000P Real time PCR System (Agilent, USA) with SYBR Green qPCR master Mix (DBI Bioscience, Germany). The relative expression levels of the selected miRNAs were detected

with a RT-PCR reaction system. The Primers used in these experiments are listed in **Table 1**.

Experimental animals

Seven-week old male Sprague Dawley (SD) rats (n=49, 180-250 g) were provided by the Animal Experimental Center of Shandong Provincial Hospital. A total of 49 rats were used for rat model construction and evaluation as follows: 15 rats were used to establish the rat model, 15 rats were injected with normal saline and served as negative control (NS) animals, and 3 rats served as blank control animals. The remaining 16 rats were used for miRNA function verification studies. All rats had free access to food and water and were kept in an air-conditioned room maintained at 20-25°C. All experimental protocols were approved by the Animal Ethics Committee of Shandong Provincial Hospital.

Autologous blood clot preparation

The rats were anesthetized by an intraperitoneal injection of 10% chloral hydrate solution (0.3 g/kg). Next, under sterile conditions, a glass capillary tube (inner diameter, 1 mm) was used to remove 0.5 mL of blood from the angular vein of each rat, and five units of thrombin were added to the collected blood. After mixing, the blood was immediately pushed into a fine polyethylene pipe and let sit overnight to form blood clots. The blood was then treated with normal saline and converted into autologous blood clots, which were subsequently trimmed to 3~4 mm in length and washed with normal saline. After repeated rinsing, the 3~4 mm clots were converted into cylindrically shaped emboli (1~2 mm in diameter and 3-4 mm in length) and stored for later use.

Establishment of the PTE model

Rats have been regarded as an optimal model for use in PTE research [19]. Rats in the experimental group were weighed and then anesthetized with an intraperitoneal injection of sodium

The role of miR-514a-5p in pulmonary thromboembolism

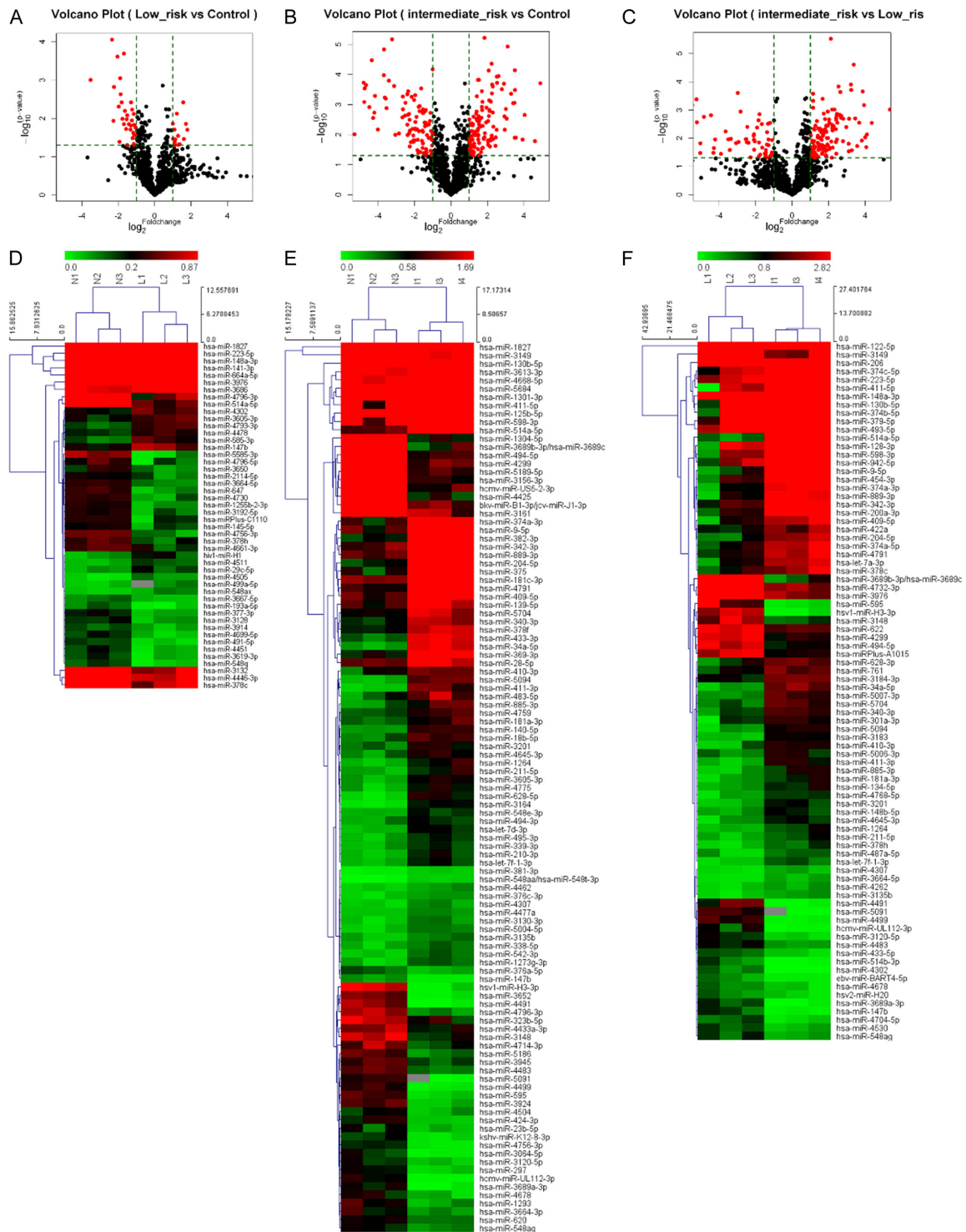


Figure 1. The unsupervised hierarchical clustering of miRNA in different groups. A-C. Volcano plots of all quantified miRNAs between low-risk PTE and normal, intermediate-risk and normal and intermediate-risk PTE and low-risk PTE groups, respectively. Red indicates the differentially expressed miRNAs and the black indicates the miRNAs without changes in expression; D-F. Heat map of the differentially expressed miRNAs between low-risk PTE and normal, intermediate-risk and normal and intermediate-risk PTE and low-risk PTE groups, respectively. Green indicates down-regulation of the corresponding gene, and red indicates up-regulation. For each type of miRNA, multiple probes were spotted on the array, and the average intensity of those probes was calculated to represent the expression level of the specific miRNA. The relative expression levels of all the differentially expressed RNAs were then clearly displayed on a hierarchical clustering heat map. The thresholds for up- and down-regulated miRNAs were a +1.5-fold and -1.5-fold change, respectively, and a p -value < 0.05.

The role of miR-514a-5p in pulmonary thromboembolism

Table 3. Alterations in plasma microRNA levels in patients with low-risk PTE compared to healthy controls (n=20)

MicroRNA	Regulation	Fold-change	p-value
hsa-miR-3976	Up	3.411	0.042
hsa-miR-4793-3p	Up	3.088	0.035
hsa-miR-3686	Up	2.807	0.023
hsa-miR-147b	Down	2.545	0.006
hsa-miR-3605-3p	Up	2.293	0.015
hsa-miR-4302	Up	2.047	0.045
hsa-miR-4478	Up	2.004	0.021
hsa-miR-1827	Down	1.912	0.043
hsa-miR-378c	Down	0.48	0.032
hsa-miR-4661-3p	Down	0.48	0.003
hsa-miR-148a-3p	Down	0.47	0.002
hsa-miR-514a-5p	Up	2.145	0.013
hsa-miR-223-5p	Down	0.42	0.018
hsa-miR-4446-3p	Down	0.42	0.036
hsa-miR-141-3p	Down	0.42	0.025
hsa-miR-664a-5p	Down	0.41	0.004
hsa-miRPlus-C11110	Down	0.4	0.003
hsa-miR-4796-3p	Down	0.36	0.034
hsa-miR-3132	Down	0.3	0.012
hsa-miR-4756-3p	Down	0.2	0.032

PTE: pulmonary thromboembolism.

pentobarbital (40 mg/kg). Next, 27~30 emboli were injected into the left external jugular vein, and the same procedure was repeated at 2 weeks after the first injection. The second injection was followed by an intramuscular injection of gentamicin (1000 units/kg, once per day) to prevent local infection. Rats in the NS group underwent the same procedures as those in the experimental group; however, they did not receive a thrombus injection. Rats in the blank control group received no treatment and did not undergo any procedures. The rats in the various groups were then further divided into the following subgroups according to the observation time: 2 week-NS, PTE subgroup; 4 week-NS, PTE subgroup; 8 week-NS, PTE subgroup.

Oligonucleotide injection

The miR-514a-5p mimic and negative control (NC) oligonucleotides were chemically synthesized by Ribobio (Guangzhou, China). To determine the function of miR-514a-5p *in vivo*, 16 rats were randomly assigned to two NS groups (n=3 per group) and two model groups (n=5 per

group), and the rats in each group were given a subcutaneous injection of miR-514a-5p mimics or the NC, respectively. The two NS groups were designated as NS + NC and NS + mimics, respectively. The two model groups were designated as PTE + NC and PTE + mimics group, respectively.

Histomorphological observations

To examine the morphology of the right ventricular and lung tissues, the heart and pulmonary tissues were surgically removed from anesthetized rats and fixed in 4% paraformaldehyde. After dehydration, the tissues were embedded in paraffin and cut into 4- μ m-thick sections for hematoxylin and eosin (H&E) staining. The sections were photographed using Motic Images Advanced 3.0 software (Motic Instruments Inc., British Columbia, Canada).

Detection of the right ventricular hypertrophy index (RVHI)

After the rats had received their different treatments, they were anesthetized, and their hearts were removed via midline thoracotomy and placed into ice-cold saline. Next, the right and left ventricles were removed from the heart and separately weighed; after which, the RVHI value was calculated according to the following formula: RVHI = the weight ratio of the right ventricle (RV) to left ventricle (LV) and interventricular septum (S): (RV/[LV+S]).

Measurement of cardiac index

To evaluate cardiac function, the rat hearts were excised and weighed; after which, the cardiac index was calculated as follows: cardiac index (%) = whole heart weight/body weight \times 100%.

Measurement of lung index

Different variables observed in sections of lung tissue (e.g., interstitial inflammation, endothelialitis, pleuritis, and thrombus formation) were measured and used to assess the degrees of lung injury. The lung index values were scored on a scale of 0-4 (0, absent; 1, mild; 2, moderate; 3, severe; 4, very severe) as previously described [22]. The total histopathological lung index value comprised the sum of the scores for all variables.

The role of miR-514a-5p in pulmonary thromboembolism

Table 4. Alterations in plasma microRNA levels in patients with intermediate-risk PTE compared to healthy controls (n=107)

MicroRNA	Regulation	Fold-change	p-value
hsa-miR-34a-5p	Up	8.71	0
hsa-miR-411-3p	Up	8.88	0.01
hsa-miR-494-5p	Down	0.37	0.01
hsa-miR-3164	Up	8.91	0.01
hsa-miR-5189-5p	Down	0.38	0.01
hsa-miR-23b-5p	Down	0.38	0.01
hsa-miR-4714-3p	Down	0.4	0.02
hsa-miR-628-5p	Up	10.1	0.03
hsa-miR-548aa/hsa-miR-548t-3p	Up	7.76	0.03
hsa-miR-3156-3p	Down	0.38	0.04
hsa-miR-3664-3p	Down	0.41	0.05
hsa-miR-3652	Down	0.04	0.03
hsa-miR-323b-5p	Down	0.43	0.02
hsa-miR-5091	Down	0.02	0.01
hsa-miR-4491	Down	0.02	0.02
hcmv-miR-UL112-3p	Down	0.04	0.03
hsa-miR-3945	Down	0.44	0.02
hsa-miR-4299	Down	0.45	0.02
hsa-miR-4433a-3p	Down	0.48	0.01
hsa-miR-1304-5p	Down	0.2	0.03
hsa-miR-4756-3p	Down	0.11	0.05
kshv-miR-K12-8-3p	Down	0.15	0.05
hsa-miR-376a-5p	Down	0.49	0.02
hsa-miR-3064-5p	Down	0.07	0.02
hsa-miR-1827	Down	0.53	0.03
hsa-miR-297	Down	0.2	0.02
hsa-miR-3924	Down	0.16	0.01
hsa-miR-548ag	Down	0.51	0.02
hsa-miR-3689a-3p	Down	0.04	0.01
hsa-miR-4499	Down	0.06	0.02
hsa-miR-424-3p	Down	0.2	0
hsv1-miR-H3-3p	Down	0.04	0.01
hsa-miR-4307	Up	2.1	0.01
bkv-miR-B1-3p/jcv-miR-J1-3p	Down	0.51	0.01
hsa-miR-620	Down	0.5	0.01
hsa-miR-181a-3p	Up	2.25	0.03
hsa-miR-3148	Down	0.34	0.04
hsa-miR-181c-3p	Up	2.29	0.02
hsa-miR-28-5p	Up	2.33	0.01
hsa-miR-3135b	Up	2.37	0.03
hsa-miR-1293	Down	0.31	0.03
hsa-miR-4759	Up	2.13	0.03
hsa-miR-338-5p	Up	2.48	0.03
hsa-miR-4477a	Up	2.01	0.03
hsa-miR-3201	Up	2.26	0.03
hsa-miR-381-3p	Up	2.73	0.03
hsa-miR-595	Down	0.12	0.03

ELISA assay

For ELISA assays, 1 mL of blood was collected from the right ventricle of an anesthetized rat and immediately centrifuged at 3000 g for 15 min. The plasma supernatant was recovered and stored at -80°C. Next, the concentrations of B-type natriuretic peptide (BNP) and the N-terminal fragment of pro-BNP (NT-pro-BNP) were measured by using commercially available ELISA kits (eBioscience, San Diego, CA, USA) according to manufacturer's protocols.

Determination of miR-514a-5p and chordin-like 1 (CHRD1) expression

After injection of the miR-514a-5p mimics, the total RNA and proteins were extracted from rat tissues using Trizol reagent (Invitrogen, Carlsbad, CA, USA) or reagents in a protein extraction kit, respectively. The primers used for miR-514a-5p, U6 RNA, CHRD1, and β -actin in the RT-PCR assays were synthesized by GeneCopoeia (Guangzhou, China). The relative expression of each gene was calculated and normalized using the $2^{-\Delta\Delta CT}$ method. For western blot studies, the total protein concentration was first determined with a BCA protein quantitation kit; after which, the proteins were separated by electrophoresis on a polyacrylamide gel and then transferred onto PVDF membranes. The membranes were then blocked with 5% skim milk, and incubated with anti-CHRD1 and anti-GAPDH antibodies. The target proteins were detected with an ECL system (Millipore, Germany) and visualized using a ChemiDoc XRS Gel Imaging system (Bio-Rad, Hercules, CA, USA). All experiments were performed in triplicate and repeated three times.

The role of miR-514a-5p in pulmonary thromboembolism

hsa-miR-3161	Down	0.36	0.03
hsa-miR-5684	Up	2.25	0.03
hsa-miR-4796-3p	Down	0.19	0.03
hsa-miR-4483	Down	0.33	0.03
hsa-miR-3120-5p	Down	0.27	0.03
hsa-miR-139-5p	Up	2.34	0.04
hsa-miR-3613-3p	Up	2.38	0.04
hsa-miR-3149	Down	0.27	0.04
hsa-miR-4462	Up	2.14	0.04
hsa-miR-147b	Down	0.2	0.04
hsa-miR-494-3p	Up	2.38	0.04
hsa-miR-1301-3p	Up	2.15	0.04
hsa-miR-125b-5p	Up	2.44	0.04
hsa-miR-5704	Up	2.35	0.04
hsa-miR-340-3p	Up	2.75	0.04
hsa-miR-378f	Up	2.81	0.04
hsa-miR-542-3p	Up	2.92	0.04
hsa-miR-4425	Down	0.26	0.04
hsa-miR-3689b-3p/hsa-miR-3689c	Down	0.21	0.04
hsa-miR-4678	Down	0.22	0.05
hsa-miR-4668-5p	Up	2.9	0.05
hsa-miR-5186	Down	0.31	0.05
hsa-miR-4504	Down	0.32	0.02
hsa-miR-339-3p	Up	2.82	0.02
hcmv-miR-US5-2-3p	Down	0.37	0.02
hsa-miR-410-3p	Up	2.49	0.02
hsa-miR-598-3p	Up	2.65	0.02
hsa-miR-4645-3p	Up	2.9	0.03
hsa-miR-548e-3p	Up	2.74	0.02
hsa-miR-376c-3p	Up	2.42	0.02
hsa-miR-1264	Up	4.18	0.02
hsa-miR-3130-3p	Up	3.01	0.02
hsa-miR-495-3p	Up	3.3	0.02
hsa-miR-3605-3p	Up	3.61	0.02
hsa-miR-889-3p	Up	2.94	0.02
hsa-let-7d-3p	Up	3.34	0.02
hsa-miR-204-5p	Up	4.41	0.02
hsa-miR-211-5p	Up	3.82	0.02
hsa-miR-409-5p	Up	3	0.02
hsa-miR-5004-5p	Up	2.94	0.02
hsa-miR-4791	Up	3.43	0.02
hsa-miR-130b-5p	Up	3.13	0.02
hsa-miR-342-3p	Up	3.41	0.03
hsa-miR-369-3p	Up	4.4	0.03
hsa-miR-433-3p	Up	5.04	0.03
hsa-miR-885-3p	Up	3.47	0.03
hsa-miR-375	Up	5.34	0.03
hsa-miR-140-5p	Up	3.55	0.03
hsa-let-7f-1-3p	Up	3.24	0.03

Statistical analysis

Quantitative results are expressed as the mean \pm standard deviation (SD) of data obtained from at least three experiments. All statistical analyses were performed using SPSS Statistics for Windows, Version 17.0 (SPSS Inc., Chicago, IL., USA). Comparisons between groups were performed by using one-way analysis of variance (ANOVA) or Student's t-test. The unpaired Student's t-test was used to analyze the expression of miRNAs in healthy and PTE groups. Two-way ANOVA was used to analyze the right ventricular hypertrophy, cardiac and lung index, the levels of BNP and NT-pro-BNP expression, and the relative expression of miR-514a-5p and CHRDL1. *P*-values < 0.05 were considered to be statistically significant.

Results

MiRNA signatures discriminated PTE tissues from paired normal tissues

To identify the miRNA signatures associated with PTE development, we performed a miRNA microarray analysis on tissues obtained from 10 PTE patients (5 low-risk PTE and 5 intermediate-risk PTE), as well as from 5 healthy control subjects (**Table 2**). The unsupervised hierarchical clustering method was used to differentiate the diseased tissues from their paired normal tissues (**Figure 1**). A fold-change > 1.5 or < 0.5 and a *p*-value < 0.05 were chosen as cut-off criteria and visualized using a Volcano Plot (**Figure 1A-C**). In total, we found 20 significantly expressed miRNAs in the low-risk PTE group (**Figure 1D**). These 20 miRNAs are listed in

The role of miR-514a-5p in pulmonary thromboembolism

hsa-miR-18b-5p	Up	3.03	0.03
hsa-miR-514a-5p	Up	4.71	0.03
hsa-miR-9-5p	Up	4.45	0.03
hsa-miR-210-3p	Up	3.79	0.04
hsa-miR-5094	Up	6.3	0.04
hsa-miR-1273g-3p	Up	3.43	0.04
hsa-miR-4775	Up	4.9	0
hsa-miR-382-3p	Up	6.01	0
hsa-miR-411-5p	Up	4.39	0
hsa-miR-483-5p	Up	3.92	0.04
hsa-miR-374a-3p	Up	4.95	0

Table 5. Alterations in plasma microRNA levels in patients with intermediate-risk PTE compared to low-risk PTE (n=83)

MicroRNA	Regulation	Fold-change	p-value
hsa-miR-411-5p	Up	43.19	0
hsa-miR-301a-3p	Up	6.82	0.01
hsa-miR-4768-5p	Up	4.18	0.01
hsa-miR-4645-3p	Up	4.41	0.01
hsa-miR-181a-3p	Up	3.75	0.01
hsa-let-7f-1-3p	Up	3.4	0.01
hsa-miR-3664-5p	Up	2.66	0.01
hsa-miR-5094	Up	4.68	0.01
hsa-miR-4307	Up	2.19	0.01
hsa-miR-4262	Up	2.2	0.01
hsa-miR-410-3p	Up	5.53	0.01
hsa-miR-3135b	Up	2.74	0.01
hsa-miR-378h	Up	3.6	0.01
hsa-miR-889-3p	Up	8.34	0.01
hsa-miR-34a-5p	Up	7.06	0.02
hsa-miR-885-3p	Up	4.7	0.02
hsa-miR-3201	Up	3.39	0.02
hsa-miR-409-5p	Up	5.84	0.02
hsa-miR-1264	Up	2.96	0.02
hsa-miR-374a-3p	Up	6.95	0.02
hsa-miR-134-5p	Up	2.81	0.02
hsa-miR-3183	Up	4.38	0.02
hsa-miR-9-5p	Up	7.38	0.03
hsa-miR-411-3p	Up	5.33	0.03
hsa-let-7a-3p	Up	4.33	0.03
hsa-miR-128-3p	Up	6.4	0.03
hsa-miR-340-3p	Up	3.15	0.03
hsa-miR-148b-5p	Up	2.52	0.03
hsa-miR-211-5p	Up	2.8	0.03
hsa-miR-598-3p	Up	5.27	0.03
hsa-miR-628-3p	Up	3.13	0.03
hsa-miR-5007-3p	Up	3.98	0.03
hsa-miR-487a-5p	Up	3.23	0.04

Table 3, and include hsa-miR-3976, hsa-miR-4793-3p, and hsa-miR-3686. A total of 107 miRNAs were significantly expressed in the intermediate-risk PTE group (**Figure 1E**). The changes in miRNA expression found in the intermediate-risk PTE group when compared with the control group are shown in **Table 4**. Furthermore, 83 mRNAs were differentially expressed in the intermediate-risk PTE group when compared with their expression in the low-risk PTE group (**Figure 1F** and **Table 5**).

Validation of candidate miRNAs

When compared with miRNAs expressed in the healthy control group, the three most up-regulated mRNAs (hsa-miR-514a-5p, hsa-miR-369-3p, and hsa-miR-885-5p) and the three most down-regulated mi-RNAs (hsa-miR-1304-5p, hsa-miR-147b, and hsa-miR-323b-5p) were found in the intermediate-risk PTE group (**Table 6**). Next, these mRNAs were validated by using RT-qPCR in a total of 20 pairs of PTE and adjacent normal clinical tissue specimens. As shown in **Figure 2**, the expression patterns of miR-514a-5p, miR-369-3p, and miR-147b were in accordance with results from the microarray assays. However, there was no significant difference in the levels of miR-885-5p, miR-1304-5p, and miR-323b-5p expression in the PTE and healthy control specimens. Notably, a microarray analysis of miRNAs revealed an obviously higher expression of miR-514a-5p in the intermediate-risk PTE group relative to that in the low-risk PTE group. Therefore, miR-514a-5p was chosen as the subsequent research target.

The role of miR-514a-5p in pulmonary thromboembolism

hsa-miR-454-3p	Up	5.04	0.04
hsa-miR-5704	Up	3.36	0.04
hsa-miR-204-5p	Up	4.4	0.04
hsa-miR-4704-5p	Down	0.22	0.04
hsa-miR-374b-5p	Up	7.23	0.04
hsa-miR-378c	Up	2.81	0.04
hsa-miR-200a-3p	Up	4.11	0.04
ebv-miR-BART4-5p	Down	0.2	0.04
hsa-miR-761	Up	2.41	0.04
hsa-miR-374a-5p	Up	3.24	0.04
hsa-miR-514a-5p	Up	11.05	0.04
hsa-miR-5006-3p	Up	2.42	0.04
hsa-miR-4678	Down	0.38	0.04
hsv2-miR-H20	Down	0.35	0.04
hsa-miR-4302	Down	0.03	0.01
hsa-miR-433-5p	Down	0.28	0.01
hsa-miR-942-5p	Up	3	0.01
hsa-miR-4791	Up	2.97	0
hsa-miR-130b-5p	Up	4.85	0.01
hsa-miR-548ag	Down	0.49	0.01
hsa-miR-4530	Down	0.42	0.01
hsa-miR-514b-3p	Down	0.06	0.01
hsa-miR-342-3p	Up	2.92	0.01
hsa-miR-147b	Down	0.09	0.01
hsa-miR-3689a-3p	Down	0.05	0.01
hsa-miR-4491	Down	0.01	0
hsa-miR-422a	Up	2.32	0
hsa-miR-4483	Down	0.4	0
hsa-miR-374c-5p	Up	3.62	0
hcmv-miR-UL112-3p	Down	0.04	0.01
hsa-miR-3184-3p	Up	2.27	0.01
hsa-miR-3120-5p	Down	0.19	0.01
hsa-miR-379-5p	Up	4.04	0.01
hsa-miR-3148	Down	0.26	0.03
hsa-miR-4499	Down	0.04	0.02
hsa-miR-223-5p	Up	2.27	0.02
hsv1-miR-H3-3p	Down	0.03	0.02
hsa-miRPlus-A1015	Down	0.39	0
hsa-miR-493-5p	Up	2.94	0.02
hsa-miR-4299	Down	0.34	0.03
hsa-miR-148a-3p	Up	2.25	0.03
hsa-miR-494-5p	Down	0.33	0.03
hsa-miR-595	Down	0.06	0.03
hsa-miR-622	Down	0.49	0.04
hsa-miR-206	Up	2.08	0.05
hsa-miR-3976	Down	0.47	0.05
hsa-miR-4732-3p	Down	0.43	0.05
hsa-miR-3689b-3p/hsa-miR-3689c	Down	0.13	0.01
hsa-miR-3149	Down	0.25	0
hsa-miR-122-5p	Up	2.47	0.02

Next, GO and pathway analyses were performed. As shown in **Figure 3A**, a cellular component analysis showed that Nucleus and Cytoplasm accounted for 66.7% and 53.3%, respectively (**Figure 3A**), while, a biological process analysis showed that the genes targeted by miR-514a-5p participated in cell communication (25%) and signal transduction (25%) (**Figure 3B**). A molecular function analysis showed that most of the molecular functions were unknown (37.5%), and GTPase activity and DNA binding accounted for 8.3% and 8.3%, respectively (**Figure 3C**). Finally, the pathway analysis showed that PI3K signaling events, the PDGFR-beta signaling pathway, ErbB1 downstream signaling, and the mTOR signaling pathway accounted for 71.4% (**Figure 3D**).

Morphological changes in the rat PTE model

We next investigated the morphological changes that occurred in the PTE rat model, as based on results shown by H&E staining. As shown in **Figure 4**, larger amounts of inflammatory exudate and infiltrated cells were accumulated in the lung tissues of all the PTE model groups when compared with the control group. Additionally, we observed disordered arrangements of myocardial fibroblasts, broadened intercellular spaces, diapedesis of erythrocytes, and lower numbers of nuclei in the right ventricular tissues of all the PTE model groups when compared with right ventricular tissues in the control group. Furthermore, these phenomena became more obvious as the thrombus time was extended.

Evaluation of the rat PTE model

Right ventricular hypertrophy, one of the consequences of

The role of miR-514a-5p in pulmonary thromboembolism

Table 6. Alterations in plasma microRNA levels in patients with PTE compared to healthy controls

MicroRNA	Regulation	Fold-change	p-value
hsa-miR-514a-5p	Up	4.713	0.003
hsa-miR-369-3p	Up	4.399	0.023
hsa-miR-885-3p	Up	3.474	0.013
hsa-miR-323b-5p	Down	0.428	0.024
hsa-miR-147b	Down	0.204	0.041
hsa-miR-1304-5p	Down	0.196	0.015

PTE: pulmonary thromboembolism.

PTE, was assessed in both the model and control groups by calculating the RVHI. As shown in **Figure 5A**, the RVHI values in the PTE group were significantly increased at 4 weeks (1.50 ± 0.18 , $P < 0.01$) and 8 weeks of PTE ($2.10 \pm 0.74\%$, $P < 0.001$) when compared those values in the NS group (1.00 ± 0.20). In addition, when compared with lung index values in the NS group (1.00 ± 0.14), the lung index values after 2 weeks of PTE (1.39 ± 0.11) and 8 weeks of PTE (1.34 ± 0.25) were significantly increased ($P < 0.01$ and $P < 0.05$, respectively). However, there was no significant difference between the cardiac index values in the NS and PTE model groups. Next, the expression levels of B-type natriuretic peptide (BNP) and the N-terminal fragment of pro-BNP (NT-pro-BNP), two well-studied biomarkers of PTE and heart failure, were evaluated by ELISA to further demonstrate the successful construction of our PTE model. As depicted in **Figure 4B**, the levels of both BNP and NT-pro-BNP were significantly elevated in the PTE model rats when compared with their levels in the NS rats, and these differences became greater as the PTE time was extended (**Figure 5B**, $*P < 0.05$, $**P < 0.01$). Together, these results suggested that the experimental PTE animal model had been successfully constructed.

Investigation of the function of miR-514a-5p in the PTE model rats

Results from our RT-PCR validation studies with PTE patients suggested that miR-514a-5p plays an important role in the occurrence of PTE. Furthermore, after injection of the miR-514a-5p mimics, the lung tissues from animals in both the NS and PTE groups exhibited an exacerbation of inflammatory phenomena when compared with lung tissues from animals

injected with the NC (**Figure 6A**). We consistently observed reduced numbers of nuclei and broader intercellular spaces in samples of right ventricular myocardium tissue from the NS + mimics group and PTE + mimics group when compared with those parameters in the NS + NC and PTE + NC groups, respectively (**Figure 6A**). Transfection with miR-514a-5p also led to significant increases in the RVHI and lung index values and BNP and NT-pro-BNP levels in rats when compared with those values and levels in rats injected with the control agents (**Figure 6B** and **6C**, $P < 0.05$, $P < 0.01$). These results demonstrated that overexpression of miR-514a-5p could contribute to the induction of PTE and exacerbate the disease *in vivo*.

MiR-514a-5p targeted CHRDL1 in the PTE rat model

MicroRNAs generally regulate target gene expression by directly binding to the 3'UTR region of the target gene's mRNA. Therefore, we used Targetscan (<http://www.targetscan.org>) to predict the target genes of miR-514a-5p. Among the various target genes, CHRDL1 has been reported to be involved in angiogenesis by regulating the balance between BMP-4 and VEGF [23]; this led us to speculate that CHRDL1 might be a target of miR-514a-5p. As shown in **Figure 7A**, a bioinformatics analysis predicted a miR-514a-5p binding site at the 3'-UTR of CHRDL1 mRNA, ranging from base sites 2888 to 2894. Moreover, the level of miR-514a-5p mRNA expression was significantly increased, but CHRDL1 expression was remarkably decreased in the NS and PTE model groups after injection of the miR-514a-5p mimics (**Figure 7B**, $P < 0.001$). The changes in CHRDL1 protein expression were consistently similar to the trends shown by RT-PCT results (**Figure 7C**, $P < 0.05$, $P < 0.01$). Collectively, the above evidence suggests that miR-514a-5p partially promotes the progression of PTE by downregulating CHRDL1 expression.

Discussion

PTE contributes to the global burden of cardiovascular disease in terms of morbidity, mortality, and financial impact on healthcare systems [20, 21] Current management strategies are tailored to the patient's risk of early death or other serious early complications [22, 23]. Risk

The role of miR-514a-5p in pulmonary thromboembolism

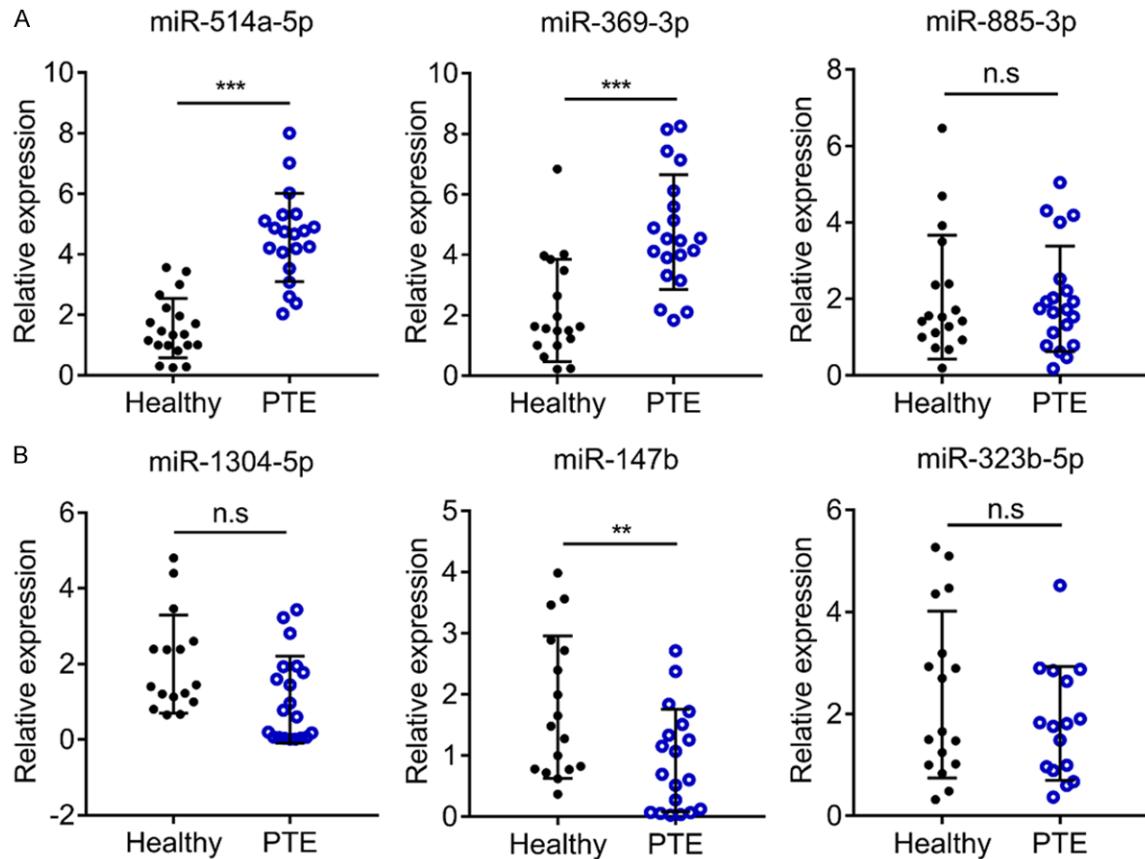


Figure 2. RT-PCR verification of six differentially expressed miRNAs in the PTE and control groups. A. MiRNAs were up-regulated in 20 pairs of diseased and adjacent normal clinical specimens, including miR-514a-5p, miR-369-3p, and miR-885-3p; B. MiRNAs were down-regulated in 20 pairs of diseased and adjacent normal clinical specimens, including miR-1304-5p, miR-147b, and miR-323b-5p; Data shown are means \pm SD; ** $P < 0.01$; *** $P < 0.001$ vs. healthy.

stratification is essential to drive clinical management via the prognosis assessment of PTE [24]. Some indicators have been used for risk stratification of PTE, and especially for PTE accompanied by RVD; these indicators include sPESI, BNP, and NT-proBNP [25, 26]. However, because of the variable clinical manifestations of PTE and the poor sensitivity of the indicators, those indicators for risk stratification of PTE remain controversial. Hence, it is very important to look for the key factors to improve the prognosis of PTE.

Recent studies have found that miRNAs play crucial roles in many cellular processes, such as proliferation, differentiation, and apoptosis [27]. MiRNAs have been intensively investigated as noninvasive biomarkers for diseases [28]. Recent studies have also explored the value of miRNAs as biomarkers for diagnosing PTE. Serum microRNA-1233, microRNA-134,

and miR-28-3p could possibly serve as specific biomarkers and potential plasma biomarkers for diagnosing PTE [16-18]. In addition, increasing numbers of studies have reported that miRNA (e.g., microRNA-27a/b and microRNA-221) was found in the expressed mRNA of PTE patients [29, 30]. In the present study, miR-514a-5p was not only significantly differentially expressed in PTE patients when compared with control subjects, but was also differentially expressed in low-risk PTE patients when compared with intermediate-risk PTE patients. PTE is a significant clinical problem that can lead to RVD [31]. BNP and NT-pro-BNP are considered as good markers for assessing RVD [32]. Up to now, miR-514a-5p has been primarily studied in cancer research. For example, miR-514a was shown to mediate expression of NF1, a tumor suppressor, and regulate the sensitivity of melanoma cell lines to BRAFi [33]. However, no study has investigated the

The role of miR-514a-5p in pulmonary thromboembolism

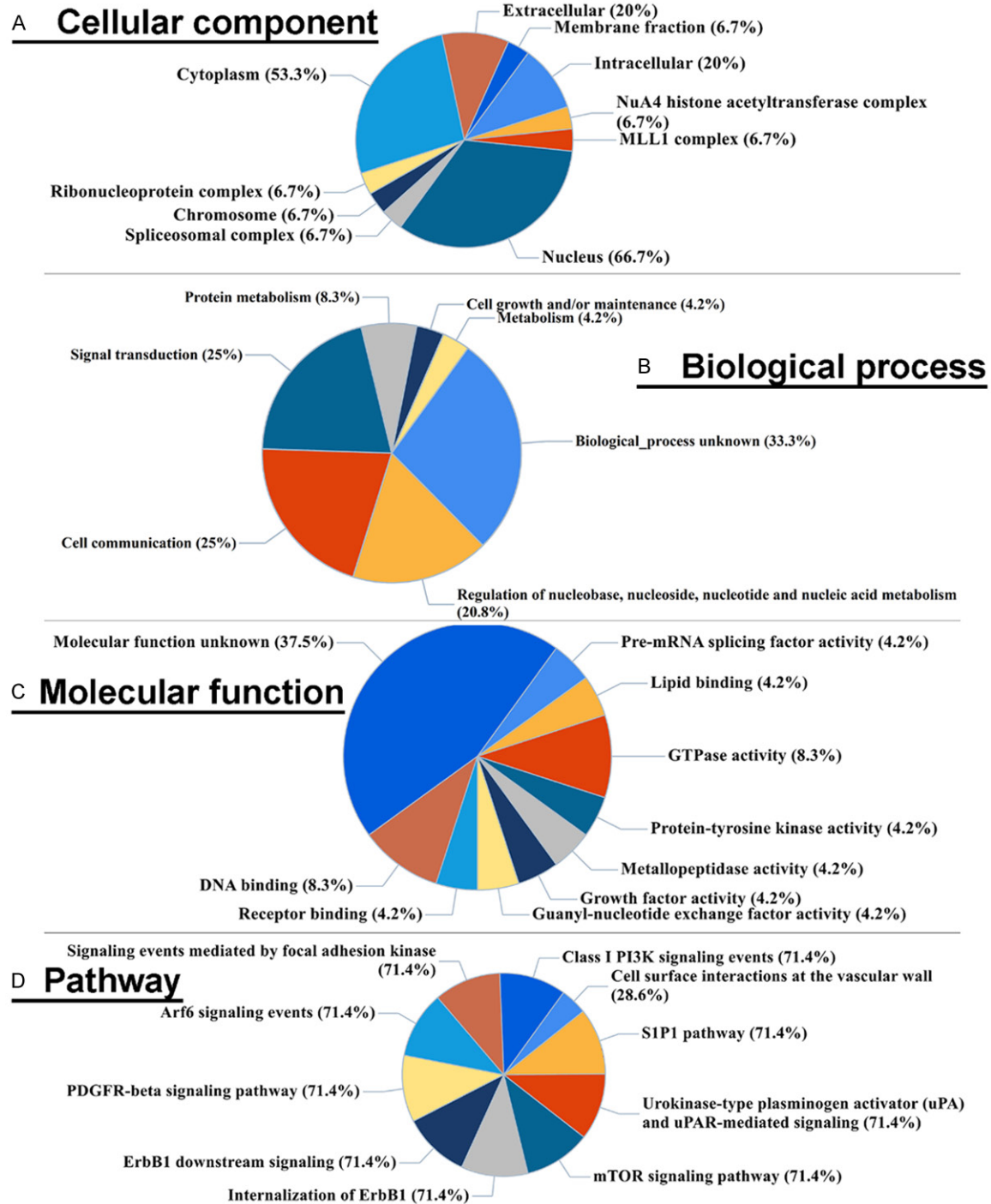


Figure 3. Go and pathway analyses of target genes of miR-514a-5p. (A-C) Go analysis including cellular component (A), biological process (B) and molecular function (C). (D) Pathway analysis. In the GO analysis, count ≥ 2 and $P \leq 0.05$ were considered to be statistically significant.

role of miR-514a-5p in PTE or another lung disease. In order to determine the value of miR-514a-5p as a prognostic factor in this study, we measured its effect on some indexes of PTE. We found that overexpression of miR-514a-5p exacerbated the inflammation in PTE rats and

increased their RVHI and lung index values, as well as their BNP and NT-Pro BNP levels. Taken together, these results suggested miR-514a-5p as a candidate molecule for use in the prognostic and risk stratification of PTE patients.

The role of miR-514a-5p in pulmonary thromboembolism

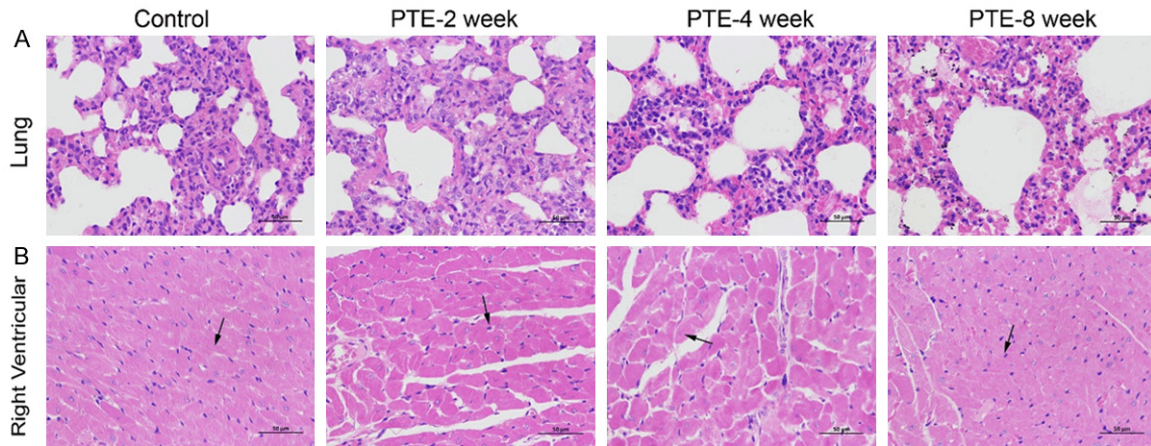


Figure 4. Morphological changes were observed in the PTE model rats. H&E staining of lung tissues (A) and right ventricular tissues (B) from all PTE model groups and control groups. Representative pictures of histopathology for lung tissues and right ventricular tissues were selected for the PTE model rats at 2-, 4-, and 8-weeks, respectively. The heart and pulmonary tissues were surgically removed from anesthetized rats and fixed in 4% paraformaldehyde. After dehydration, the tissues were embedded in paraffin and cut into 4- μ m-thick sections for hematoxylin and eosin (H&E) staining. The sections were photographed using Motic Images Advanced 3.0 software. Magnification, \times 200.

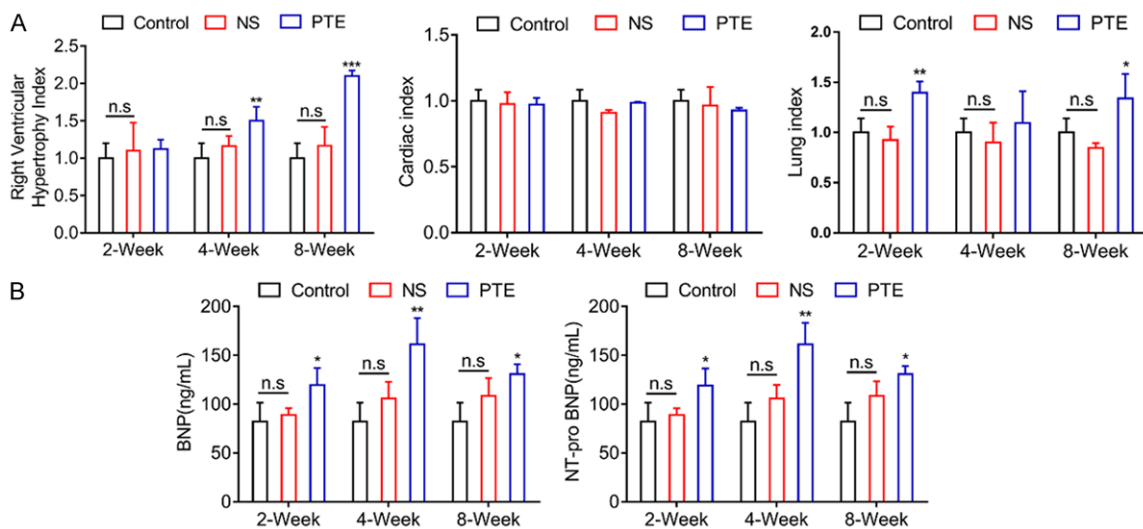


Figure 5. The established rat PTE model was evaluated in vivo. A. Dynamic changes in the mean right ventricular hypertrophy index (RVHI), cardiac index, and lung index in the PTE model rats at 2-, 4-, and 8-weeks, respectively. B. Expression of BNP and NT-pro-BNP in the PTE model rats at 2-, 4-, and 8-weeks, respectively, and in the normal saline (NS) groups, as detected by ELISA. Data represent the mean \pm SD; n.s.; not significant; *, ** and *** indicate $P < 0.05$; $P < 0.01$; $P < 0.001$, respectively, vs. NS; # and ## indicate $P < 0.05$ and $P < 0.01$, respectively, vs. PTE + NC.

Previous studies have shown that right ventricular dysfunction is one of the most common causes of clinical worsening and death among PTE patients [34, 35], and BNP and NT-proBNP have been widely used as indicators of heart failure [36]. Although the prognostic value of RVD for PTE patients remains controversial, gaining a better understanding of the mechanism that leads to RVD in intermediate-risk PTE

patients should improve the interventions for used for PTE. However, at present, few studies have focused on the mechanism of PTE or the mechanism that leads to RVD in PTE patients, Sutendra *et al.* [37] demonstrated that a decrease in the levels of angiogenic factors and angiogenesis can potentiate the remodeling of right ventricular hypertrophy in cases of pulmonary arterial hypertension. However, no

The role of miR-514a-5p in pulmonary thromboembolism

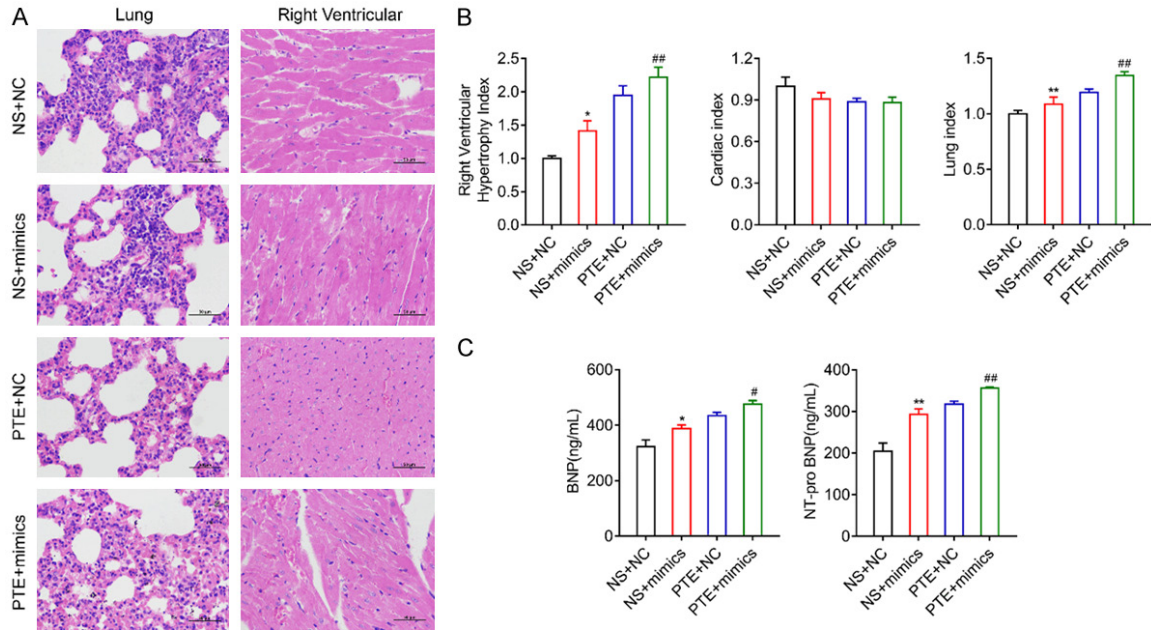


Figure 6. MiR-514a-5p exacerbated the development of PTE *in vivo*. A. H&E staining of lung tissues and right ventricular tissues from control rats and PTE rats after injection with miR-514a-5p mimics or the NC, respectively. B. Dynamic changes in the mean right ventricular hypertrophy index (RVHI), cardiac index, and lung index in the normal saline (NS) and PTE model rats after injection with miR-514a-5p mimics or the NC, respectively. C. Expression of BNP and NT-pro-BNP in NS rats and PTE model rats, respectively, after injection with miR-514a-5p mimics or the NC. Data represent the mean \pm SD; *: control + NC vs. control + mimics; #: PTE + NC vs. PTE + mimics; * $P < 0.05$; *** $P < 0.001$; ## $P < 0.01$; ### $P < 0.001$.

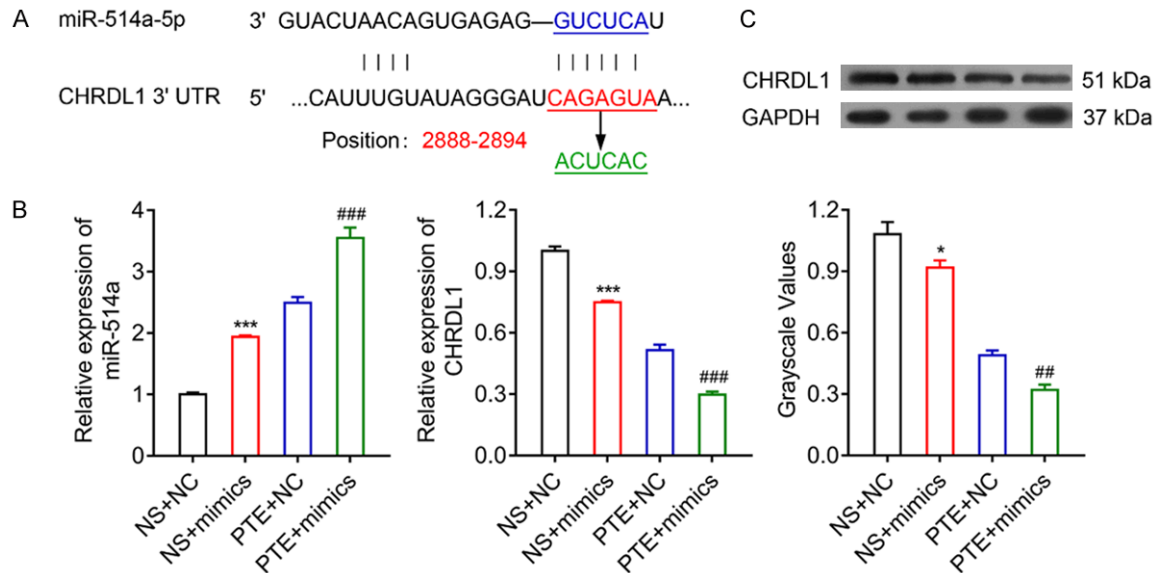


Figure 7. MiR-514a-5p targets the 3'-UTR of CHRDL1 to inhibit its expression. A. Bioinformatics analyses showing the binding of miR-514a-5p to the 3'-UTR of CHRDL1 mRNA. B. The levels of miR-514a-5p and CHRDL1 mRNA as measured by qRT-PCR in tissues from rats in the normal saline (NS) group and PTE model group after injection with miR-514a-5p mimics or the NC. C. The levels of CHRDL1 protein as measured by western blot and the grayscale values as measured by image J in tissues from rats in the normal saline (NS) group and PTE model group after injection with miR-514a-5p mimics or the NC. GAPDH served as an internal standard. Data represent the \pm SD; *: NS + NC vs. NS + mimics; #: PTE + NC vs. PTE + mimics; * $P < 0.05$; ** $P < 0.01$ vs. NS + NC group; ### $P < 0.01$; #### $P < 0.001$ vs. PTE + NC group.

report has addressed the relationship between *CHRD1* and RDV. However, we previously found that *CHRD1* is involved in angiogenesis by regulating the balance between BMP-4 and VEGF [38, 39]. Therefore, we hypothesize that *CHRD1* might participate in the development of RDV by affecting angiogenesis. In this study, BNP and NT-pro BNP levels were found to be increased in the PTE and miR-514a-5p groups, and were further enhanced in PTE animals that were administered miR-514a-5p. Additionally, these results demonstrated that *CHRD1* might be involved in RVD caused by PTE. In this study, we identified a miR-514a-5p binding site in the 3'-UTR of *CHRD1* mRNA, and found that *CHRD1* mRNA levels were significantly down-regulated in the miR-514a-5p mimics groups, suggesting that *CHRD1* might be regulated by miR-514a-5p. However, whether miR-514a-5p affects the RVD process of PTE by down-regulating *CHRD1* remains to be verified.

Conclusion

In conclusion, miR-514a-5p was able to potentiate PTE development by promoting inflammation, lung injury, and also right ventricular hypertrophy and dysfunction. MiR-514a-5p might participate in these processes by regulating expression of the *CHRD1* gene. Although the mechanism of miR-514a-5p requires further study, our findings provide a solid foundation for utilizing miRNAs in the prognosis of PTE, and suggest miR-514a-5p as a novel target for intervention in PTE.

Acknowledgements

This research was supported by the Natural Science Foundation of Shandong Province (ZR2014HM083).

Disclosure of conflict of interest

None.

Abbreviations

BNP, B-type natriuretic peptide; *CHRD1*, Chordin-like 1; NC, negative control; NS, normal saline; NT-pro-BNP, N-terminal fragment of pro-BNP; PTE, pulmonary thromboembolism; RVD, right ventricular dysfunction; RVHI, right ventricular hypertrophy index; sPESI, simplified pulmonary embolism severity index.

Address correspondence to: Dr. Ling Zhu, Department of Respiratory Medicine, Shandong Provincial Hospital Affiliated to Shandong University, 9677 Jingshi Road, Jinan 250000, Shandong, China. Tel: +86 0531 68773268; E-mail: zhuling7103@163.com; Dr_Zhu939@126.com

References

- [1] Kline JA and Kabrhel C. Emergency evaluation for pulmonary embolism, part 1: clinical factors that increase risk. *J Emerg Med* 2015; 48: 771-780.
- [2] Lee K, Kwon O, Lee EJ, Sin MJ, Lee JS, Lee S, Kang DH, Song JK and Song JM. Prognostic value of echocardiographic parameters for right ventricular function in patients with acute non-massive pulmonary embolism. *Heart Vessels* 2019; 34: 1187-1195.
- [3] Hsu N, Wang T, Friedman O and Barjaktarevic I. Medical management of pulmonary embolism: beyond anticoagulation. *Tech Vasc Interv Radiol* 2017; 20: 152-161.
- [4] Barrios D, Morillo R, Lobo JL, Nieto R, Jaureguizar A, Portillo AK, Barbero E, Fernandez-Golfín C, Yusen RD, Jiménez D; PROTECT investigators. Assessment of right ventricular function in acute pulmonary embolism. *Am Heart J* 2017; 185: 123-129.
- [5] Vitarelli A, Barilla F, Capotosto L, D'Angeli I, Truscetti G, De Maio M and Ashurov R. Right ventricular function in acute pulmonary embolism: a combined assessment by three-dimensional and speckle-tracking echocardiography. *J Am Soc Echocardiogr* 2014; 27: 329-338.
- [6] Zhu L, Wang C, Yang YH, Wu YF and Zhai ZG. Prognostic value of right ventricular dysfunction and derivation of a prognostic model for patients with acute pulmonary thromboembolism. *Zhonghua Liu Xing Bing Xue Za Zhi* 2009; 30: 184-188.
- [7] Ahn S, Lee YS, Kim WY, Lim KS and Lee JL. Prognostic value of treatment setting in patients with cancer having pulmonary embolism: comparison with the pulmonary embolism severity index. *Clin Appl Thromb Hemost* 2017; 23: 615-621.
- [8] Grimson A, Farh KK, Johnston WK, Garrett-Engle P, Lim LP and Bartel DP. MicroRNA targeting specificity in mammals: determinants beyond seed pairing. *Mol Cell* 2007; 27: 91-105.
- [9] Esquela-Kerscher A and Slack FJ. Oncomir-microRNAs with a role in cancer. *Nat Rev Cancer* 2006; 6: 259-269.
- [10] Miao R, Wang Y, Wan J, Leng D, Gong J, Li J, Liang Y, Zhai Z and Yang Y. Microarray expression profile of circular RNAs in chronic throm-

The role of miR-514a-5p in pulmonary thromboembolism

- boembolic pulmonary hypertension. *Medicine (Baltimore)* 2017; 96: e7354.
- [11] Miao R, Dong XB, Gong JN, Li JF, Pang WY, Liu YY and Yang YH. Analysis of significant microRNA associated with chronic thromboembolic pulmonary hypertension. *Zhonghua Yi Xue Za Zhi* 2018; 98: 1397-1402.
- [12] Deng HY, Li G, Luo J, Wang ZQ, Yang XY, Lin YD and Liu LX. MicroRNAs are novel non-invasive diagnostic biomarkers for pulmonary embolism: a meta-analysis. *J Thorac Dis* 2016; 8: 3580-3587.
- [13] Schulte C, Karakas M and Zeller T. microRNAs in cardiovascular disease-clinical application. *Clin Chem Lab Med* 2017; 55: 687-704.
- [14] Chen Z, Nakajima T, Tanabe N, Hinohara K, Sakao S, Kasahara Y, Tatsumi K, Inoue Y and Kimura A. Susceptibility to chronic thromboembolic pulmonary hypertension may be conferred by miR-759 via its targeted interaction with polymorphic fibrinogen alpha gene. *Hum Genet* 2010; 128: 443-452.
- [15] Guo L, Yang Y, Liu J, Wang L, Li J, Wang Y, Liu Y, Gu S, Gan H, Cai J, Yuan JX, Wang J and Wang C. Differentially expressed plasma microRNAs and the potential regulatory function of Let-7b in chronic thromboembolic pulmonary hypertension. *PLoS One* 2014; 9: e101055.
- [16] Kessler T, Erdmann J, Vilne B, Bruse P, Kurovski V, Diemert P, Schunkert H and Sager HB. Serum microRNA-1233 is a specific biomarker for diagnosing acute pulmonary embolism. *J Transl Med* 2016; 14: 120.
- [17] Xiao J, Jing ZC, Ellinor PT, Liang D, Zhang H, Liu Y, Chen X, Pan L, Lyon R, Liu Y, Peng LY, Liang X, Sun Y, Popescu LM, Condorelli G and Chen YH. MicroRNA-134 as a potential plasma biomarker for the diagnosis of acute pulmonary embolism. *J Transl Med* 2011; 9: 159.
- [18] Zhou X, Wen W, Shan X, Qian J, Li H, Jiang T, Wang W, Cheng W, Wang F, Qi L, Ding Y, Liu P, Zhu W and Chen Y. MiR-28-3p as a potential plasma marker in diagnosis of pulmonary embolism. *Thromb Res* 2016; 138: 91-95.
- [19] Zagorski J and Kline JA. Differential effect of mild and severe pulmonary embolism on the rat lung transcriptome. *Respir Res* 2016; 17: 86.
- [20] Saar JA, Maack C; European Society of Cardiology. Diagnosis and management of acute pulmonary embolism. ESC guidelines 2014. *Herz* 2015; 40: 1048-1054.
- [21] Dentali F, Di Micco G, Giorgi Pierfranceschi M, Gussoni G, Barillari G, Amitrano M, Fontanella A, Lodigiani C, Guida A, Visona A, Monreal M and Di Micco P. Rate and duration of hospitalization for deep vein thrombosis and pulmonary embolism in real-world clinical practice. *Ann Med* 2015; 47: 546-554.
- [22] Bikdeli B, Wang Y, Mingos KE and Desai NR. Hospitalizations, therapies, and outcomes of pulmonary embolism in medicare beneficiaries: trends are similar to europe. *J Am Coll Cardiol* 2016; 67: 2559-2560.
- [23] Konstantinides SV. Trends in pulmonary embolism outcomes: are we really making progress? *J Am Coll Cardiol* 2016; 67: 171-173.
- [24] Werth S, Kamvissi V, Stange T, Kuhlisch E, Weiss N and Beyer-Westendorf J. Outpatient or inpatient treatment for acute pulmonary embolism: a retrospective cohort study of 439 consecutive patients. *J Thromb Thrombolysis* 2015; 40: 26-36.
- [25] den Exter PL, Zondag W, Klook FA, Brouwer RE, Dolsma J, Eijsvogel M, Faber LM, van Gerwen M, Grootenboers MJ, Heller-Baan R, Hovens MM, Jonkers GJ, van Kralingen KW, Melissant CF, Peltenburg H, Post JP, van de Ree MA, Vlasveld LT, de Vreede MJ, Huisman MV; Vesta Study Investigators. Efficacy and safety of outpatient treatment based on the hestia clinical decision rule with or without N-terminal pro-brain natriuretic peptide testing in patients with acute pulmonary embolism. A randomized clinical trial. *Am J Respir Crit Care Med* 2016; 194: 998-1006.
- [26] Lankeit M, Jimenez D, Kostrubiec M, Dellas C, Kuhnert K, Hasenfuss G, Pruszczyk P and Konstantinides S. Validation of N-terminal pro-brain natriuretic peptide cut-off values for risk stratification of pulmonary embolism. *Eur Respir J* 2014; 43: 1669-1677.
- [27] Bartel DP and Chen CZ. Micromanagers of gene expression: the potentially widespread influence of metazoan microRNAs. *Nat Rev Genet* 2004; 5: 396-400.
- [28] Pritchard CC, Cheng HH and Tewari M. MicroRNA profiling: approaches and considerations. *Nat Rev Genet* 2012; 13: 358-369.
- [29] Wang Q, Ma J, Jiang Z, Wu F, Ping J and Ming L. Diagnostic value of circulating microRNA-27a/b in patients with acute pulmonary embolism. *Int Angiol* 2018; 37: 19-25.
- [30] Liu T, Kang J and Liu F. Plasma levels of microRNA-221 (miR-221) are increased in patients with acute pulmonary embolism. *Med Sci Monit* 2018; 24: 8621-8626.
- [31] Lualdi JC and Goldhaber SZ. Right ventricular dysfunction after acute pulmonary embolism: pathophysiologic factors, detection, and therapeutic implications. *Am Heart J* 1995; 130: 1276-1282.
- [32] Klook FA, Mos IC and Huisman MV. Brain-type natriuretic peptide levels in the prediction of adverse outcome in patients with pulmonary embolism: a systematic review and meta-analysis. *Am J Respir Crit Care Med* 2008; 178: 425-430.

The role of miR-514a-5p in pulmonary thromboembolism

- [33] Stark MS, Bonazzi VF, Boyle GM, Palmer JM, Symmons J, Lanagan CM, Schmidt CW, Herington AC, Ballotti R, Pollock PM and Hayward NK. miR-514a regulates the tumour suppressor NF1 and modulates BRAFi sensitivity in melanoma. *Oncotarget* 2015; 6: 17753-17763.
- [34] Kasper W, Konstantinides S, Geibel A, Tiede N, Krause T and Just H. Prognostic significance of right ventricular afterload stress detected by echocardiography in patients with clinically suspected pulmonary embolism. *Heart* 1997; 77: 346-349.
- [35] McConnell MV, Solomon SD, Rayan ME, Come PC, Goldhaber SZ and Lee RT. Regional right ventricular dysfunction detected by echocardiography in acute pulmonary embolism. *Am J Cardiol* 1996; 78: 469-473.
- [36] Takahama H, Takashio S, Nishikimi T, Hayashi T, Nagai-Okatani C, Nakagawa Y, Amaki M, Ohara T, Hasegawa T, Sugano Y, Kanzaki H, Yasuda S, Kangawa K, Minamino N and Anzai T. Ratio of pro-B-type natriuretic peptide (BNP) to total BNP is decreased in mild, but not severe, acute decompensated heart failure patients: a novel compensatory mechanism for acute heart failure. *Int J Cardiol* 2018; 258: 165-171.
- [37] Sutendra G, Dromparis P, Paulin R, Zervopoulos S, Haromy A, Nagendran J and Michelakis ED. A metabolic remodeling in right ventricular hypertrophy is associated with decreased angiogenesis and a transition from a compensated to a decompensated state in pulmonary hypertension. *J Mol Med (Berl)* 2013; 91: 1315-1327.
- [38] Kane R, Godson C and O'Brien C. Chordin-like 1, a bone morphogenetic protein-4 antagonist, is upregulated by hypoxia in human retinal pericytes and plays a role in regulating angiogenesis. *Mol Vis* 2008; 14: 1138-48.
- [39] Gerhardt H, Golding M, Fruttiger M, Ruhrberg C, Lundkvist A, Abramsson A, Jeltsch M, Mitchell C, Alitalo K, Shima D and Betsholtz C. VEGF guides angiogenic sprouting utilizing endothelial tip cell filopodia. *J Cell Biol* 2003; 161: 1163-1177.